Source reconstruction of the 1969 Majene, Sulawesi earthquake and tsunami: A preliminary study

IOP Conf. Series: Earth and Environmental Science **873** (2021) 012054 doi:10.1088/1755-1315/873/1/012054

Source reconstruction of the 1969 Majene, Sulawesi earthquake and tsunami: A preliminary study

I.R. Pranantyo[1,4,*], A. Cipta[2], H.A. Shiddiqi[3], M. Heidarzadeh[1]

[1] Department of Civil and Environmental Engineering, Brunel University London, Uxbridge UB8 3PH, United Kingdom
[2] Geological Agency of Indonesia, Bandung, Indonesia
[3] Department of Earth Science, University of Bergen, Bergen, Norway
[4] Present: Bandung, Indonesia

E-mail: *ignatiusryanpranantyo@gmail.com

Abstract. We studied the February 23rd, 1969 M7.0 Majene, Sulawesi earthquake and tsunami. It was followed by tsunami reported at five locations. At least 64 people were killed and severe damage on infrastructures were reported in Majene region. Based on damage data, we estimated that the maximum intensity of the earthquake was MMI VIII. Focal mechanisms, derived using first motion polarity analysis, indicated that the earthquake had a thrust mechanism. Furthermore, we built hypothetical earthquake scenarios based on a rectangular fault plane of 40 km × 20 km with a homogeneous slip model of 1.5 m. We run the Open Quake and the JAGURS code to validate the macroseismic and tsunami observation data, respectively. Our best-fitted earthquake model generates maximum intensity of 8+ which is in line with the reported macroseismic data. However, the maximum simulated tsunami height from all scenario earthquakes is 2.25 m which is smaller than the 4 m tsunami height observed at Pelattoang. The possibility of contribution of another mechanism to tsunami generation requires further investigation.

Keywords: Eastern Indonesia, Sulawesi, Earthquake, Tsunami, Numerical Simulations

1. Introduction

Sulawesi Island was composed by few terranes, both detached from Australian and Eurasian plates, making the island tectonically very active, with the most prominent active fault is the Palu Koro Fault Zone [1] (Figure 1). As a result, the island is seismically active and is exposed to tsunami hazard (e.g. Cipta et al., [2], Prasetya et al., [3], Horspool et al., [4]). A deadly earthquake and tsunami occurred on 23rd February 1969 that devastated Majene region, west coast of Sulawesi (Figure 1). The Mw7.0 quake intensely jolted the region of Majene and generated a 4 m tsunami wave at Pelattoang (Figure 1c) [5, 6]. Here we conducted preliminary study on this event to understand the main generation mechanism of the earthquake and tsunami. This study would encourage further investigation to increase earthquake and tsunami resilience for Sulawesi.

2. Historical accounts

Historical accounts in Indonesia were mostly available on a description data-types and incomplete (e.g. [7, 8, 9]). For the 1969 Majene, Sulawesi event, historical accounts were available from

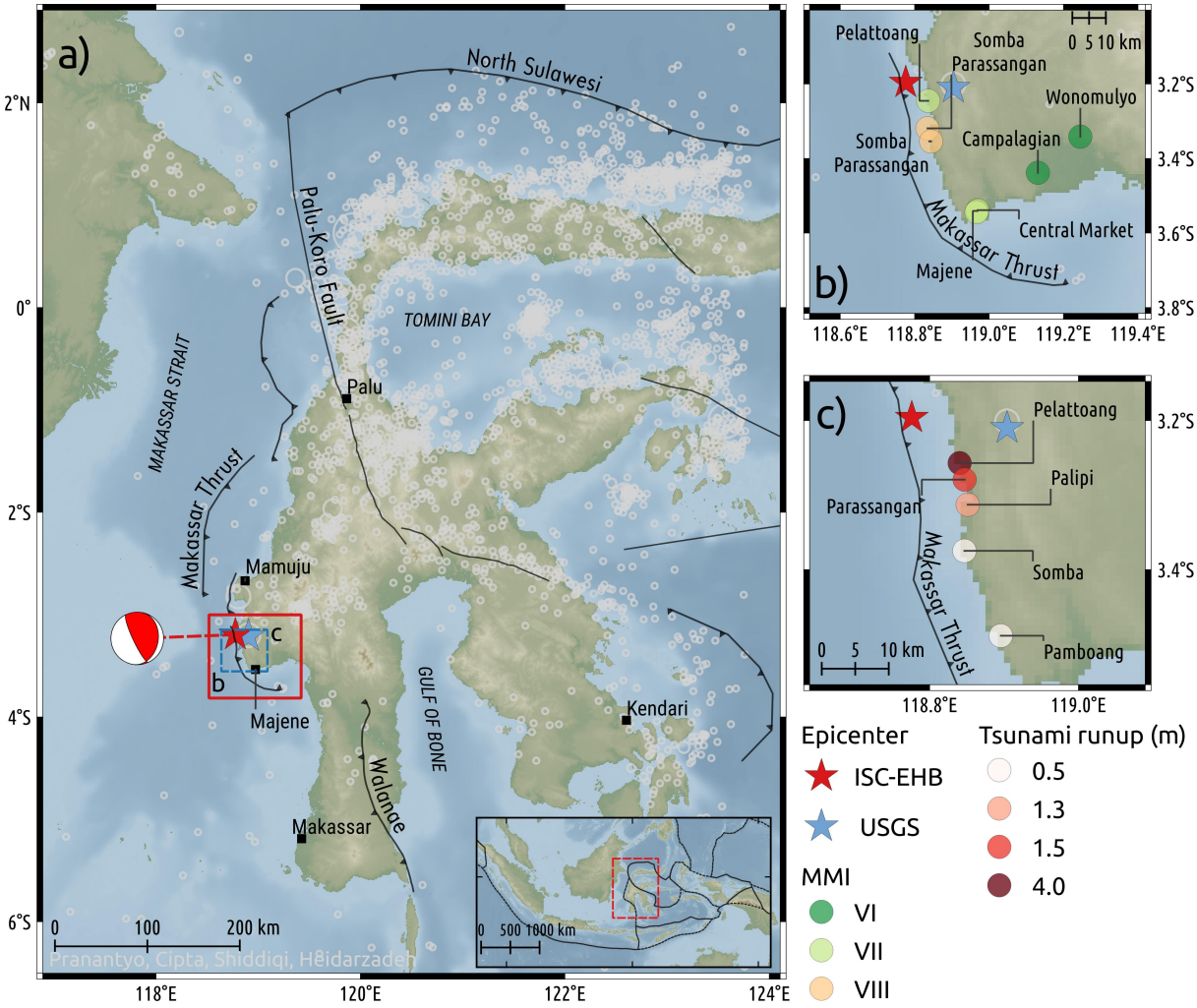

Figure 1. a) Tectonic setting of Sulawesi Island. Red and blue stars indicate the epicentre of the 1969 Majene, Sulawesi earthquake taken from the ISC-EHB and USGS catalogue, respectively. Focal mechanism is based on the first motion polarity analysis (Section 3). The red and blue boxes are inset maps for b) interpreted macroseismic data in Modified Mercalli Intensity (MMI) scales and c) tsunami height observations, respectively.

Soloviev et al., [10], Soetardjo et al., [11], Fikrie and Hardiansya, [12], and International Tsunami Information Center (ITIC) [5, 6]. Further, we converted pieces of information on infrastructure damage, land morphology changes (e.g. rockfalls, landslides, ground cracking), and ground shaking intensity felt by eyewitnesses from several locations into a Modified Mercalli Intensity (MMI) scale (Figure 1b). The data indicate that the earthquake generated massive strong motion with MMI up to VIII at Somba-Parassangan. Tsunami height observations were available at five locations ranging from 0.5 m at Pamboang to 4 m at Pellatoang (Figure 1c). Unfortunately, neither earthquake accounts from locations that were further away from the epicentre nor the estimated tsunami arrival time were available.

3. First motion polarity analysis

Earthquake location and its mechanism are important parameters in this study. According to the ISC-EHB [13] and the USGS earthquake catalogues, their earthquake epicentres are located

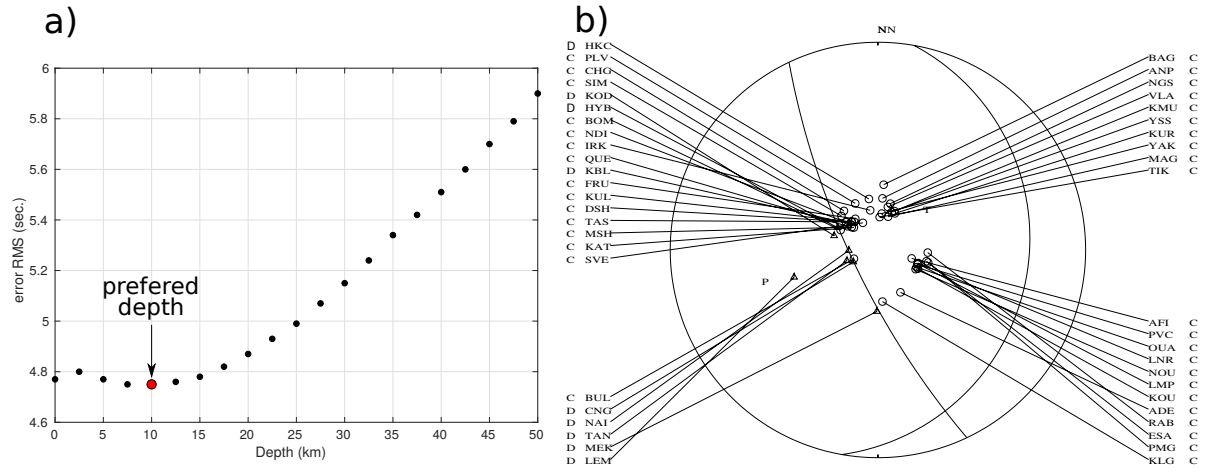

Figure 2. a) The plot of error RMS for various focal depth. The depth with lowest RMS error is marked by the red circle. b) Focal mechanism of the M7.0 1969 Majene, Sulawesi earthquake. Polarities are plotted within the lower hemisphere projection where the compression (C) and dilatation (D) are marked as small triangles and small circles, respectively.

at about 15–20 km distance apart (Figure 1a) with the earthquake depth is between 15 km and 50.4 km. Since this area is situated far from active tectonic margin, it is most likely that the Majene 1969 event was sourced from a shallow crustal fault. Therefore, we re-analysed the earthquake depth using arrival time data from ISC-EHB catalogue. We used direct P- and S-phases, as well as depth- (pP) and mantle-phases (PP, SS, and PcP) from stations at regional and teleseismic distances. Observations with very large residuals are removed. We performed a grid-search by varying the earthquake depth and fixing its epicentre by using the RMSDEP program from the SEISAN package [14, 15]. We used depth range from 0 km to 50 km, with an interval of 2.5 km. The travel times are computed using the iasp91 velocity model [16]. The travel-times error in the root-mean-square (RMS) for each depth is calculated. We found out that the depth of 10 km gives the lowest error RMS (Figure 2a). Furthermore, we utilized the FPFIT software [17] to determine the earthquake focal mechanism based on its first motion polarities reported in the ISC-EHB catalogue. A thrust mechanism was obtained with two possible focal mechanism; Strike1/Dip1/Rake1 (FM1): 10°/18°/124° and Strike2/Dip2/Rake2 (FM2): 155°/75°/80° (Figure 2b).

4. Ground motion and tsunami modelling

4.1. Scenarios and model setup

From the results above, we tested five selected scenarios (Figure 3a, Table 1 to validate the MMI (Figure 3b). We conducted ground motion (GM) modelling using the OpenQuake[1] software [18]. The software calculates peak ground acceleration (PGA) according to the ground motion prediction equation (GMPE) of Boore et al., [19] and Vs30 of Cipta et al., [2], estimated based on geological and topographic parameters. Earthquake intensity (MMI) is obtained by converting the estimated PGA using the Worden et al., [20] formula. We also performed 2D numerical tsunami propagation modelling using the JAGURS[2] code [21] to verify the tsunami height data (Figure 3b, c). We solved the non-linear shallow water wave equations. For this study, we built

[1] https://www.globalquakemodel.org/openquake, last accessed 5 October 2020
[2] https://github.com/jagurs-admin/jagurs, last accessed 10 September 2020

a digital elevation model (DEM[3]) by combining the national bathymetry (DEMNAS), contours of shallow coastal area (LPI) as well as topography (RBI) then interpolated with a resolution of 0.00225° (∼250 m). For this study, we did not conduct inundation modelling.

We assumed a rectangular fault plane model of 40 km × 20 km (based on equations from Wells and Coppersmith, [22]) with the earthquake epicentre was assumed to be the centroid of the fault plane. Firstly, we used the earthquake epicentre from the USGS catalogue with two different solutions from the first motion polarity analysis (the FM1 and FM2), referred to as USGS-FM1 and USGS-FM2. Then we also tested the epicentre from ISC-EHB catalogue, EHB-FM1 and EHB-FM2. Lastly, we applied a trial-and-error approach by shifting the earthquake location as well as changed the mechanism, Majene1969, to find the best-fit model that describes the MMI and tsunami observation data.

Table 1. Selected earthquake and tsunami scenarios to validate the 1969 Majene, Sulawesi event

Scenario	Epicentre	Coordinate*	Strike	Dip	Rake
USGS-FM1	118.9040°E, 3.2010°S	118.8041°E, 3.2751°S, 6.91 km	10°	18°	124°
USGS-FM2	118.9040°E, 3.2010°S	118.8871°E, 3.1091°S, 0.34 km	155°	75°	80°
EHB-FM1	118.7790°E, 3.1960°S	118.6761°E, 3.2701°S, 6.91 km	10°	18°	124°
EHB-FM2	118.7790°E, 3.1960°S	118.7591°E, 3.1041°S, 0.34 km	155°	75°	80°
Majene1969	118.5760°E, 3.1960°S	118.6012°E, 3.4676°S, 2.00 km	13°	15°	67°

Fault length × width = 40 km × 20 km; Homogeneous slip = 1.5 m
*top-right coordinate (longitude, latitude, top-depth) of the fault plane

4.2. Results and analysis

Firstly, by considering the tectonic setting of Sulawesi, the FM1 is the most plausible solution of the earthquake mechanism due to its North-South orientation. The closest structure to the earthquake epicentre is the Makassar Thrust (Figure 1). Therefore, we could eliminate the possibility of the USGS-FM2 and EHB-FM2 scenarios.

Second, the USGS earthquake epicentre was located on land. The GM model of the USGS-FM1 indicates the maximum MMI is a little bit further east compared to the data. Moreover, with an epicentre on land, it caused little earthquake deformation on the sea (Figure 3). Therefore, the maximum tsunami amplitude on the coastline is just a little more than ∼0.5 m, which is much lower than the 4 m observation height. On the other hand, the ISC-EHB earthquake epicentre was located on the sea. The GM model of the EHB-FM1 shows a relatively good fit for MMI compared to the data. With half of the earthquake deformation occurred on the sea, it increases the maximum tsunami height to ∼1.5 m. Unfortunately, it is still 2.5 m less than the maximum observation.

The USGS-FM1 and EHB-FM1 models produced extremely high MMI in coastal areas near fault and extending further eastward on land. On the contrary, the USGS-FM2 and EHB-FM2 scenarios, the high MMI area was suffered only at the near-fault coastal area, as expected by macroseismic data. However in the southern part of Majene, the predicted intensity was rather lower than expected. In order to obtain better model for MMI data and tsunami

[3] DEM is combination of DEMNAS (https://tides.big.go.id/DEMNAS, last accessed 10 September), LPI and RBI (https://portal.ina-sdi.or.id/downloadaoi, last accessed 10 September 2020)

height, we modified EHB-FM1 model. Based on the ISC-EHB earthquake epicentre, then we subjectively conducted a trial-and-error approach to find the most plausible earthquake location and mechanism. In this study, we found that the Majene1969 scenario is the best model to reproduce the MMI data (Figure 3). The earthquake location is slightly further west than the EHB-FM1 model with a shallower depth. The Majene1969 scenario increases the maximum simulated tsunami height to ∼2.25 m. Likely, the previous scenarios, this model still cannot fit the maximum tsunami height observation.

The observed tsunami height data has a narrow band of maximum tsunami height over 5 km distance along the coastline (Figure 1, 3). The tsunami height then significantly decreases to southward direction. It is likely that the 4 m tsunami height could be due to a local phenomenon such as an underwater landslide induced by the earthquake. However, it would need further investigation to locate where, when, and how large such a phenomenon would be.

5. Summary

We have shown preliminary result of the earthquake and tsunami source reconstruction for the 1969 Majene, Sulawesi event. We collected historical accounts of earthquake intensities and tsunami heights observation from various references. First motion polarity analysis indicates it was a thrust earthquake with the Makassar Thrust as the closest fault to the earthquake epicentre. Majority of the earthquake rupture need to be located on the sea to fit the MMI data and increase the maximum simulated tsunami height. However, all scenarios considered in this study are still unable to reproduce the 4 m tsunami height observed at Pellatoang. We assume that a local phenomenon such as a submarine landslide triggered by the earthquake was involved in the tsunami generation process. Further investigation is needed to determine the parameters of a potential landslide.

Acknowledgment

This study is supported by the Royal Society, UK (grant number CHL\R1\180173)

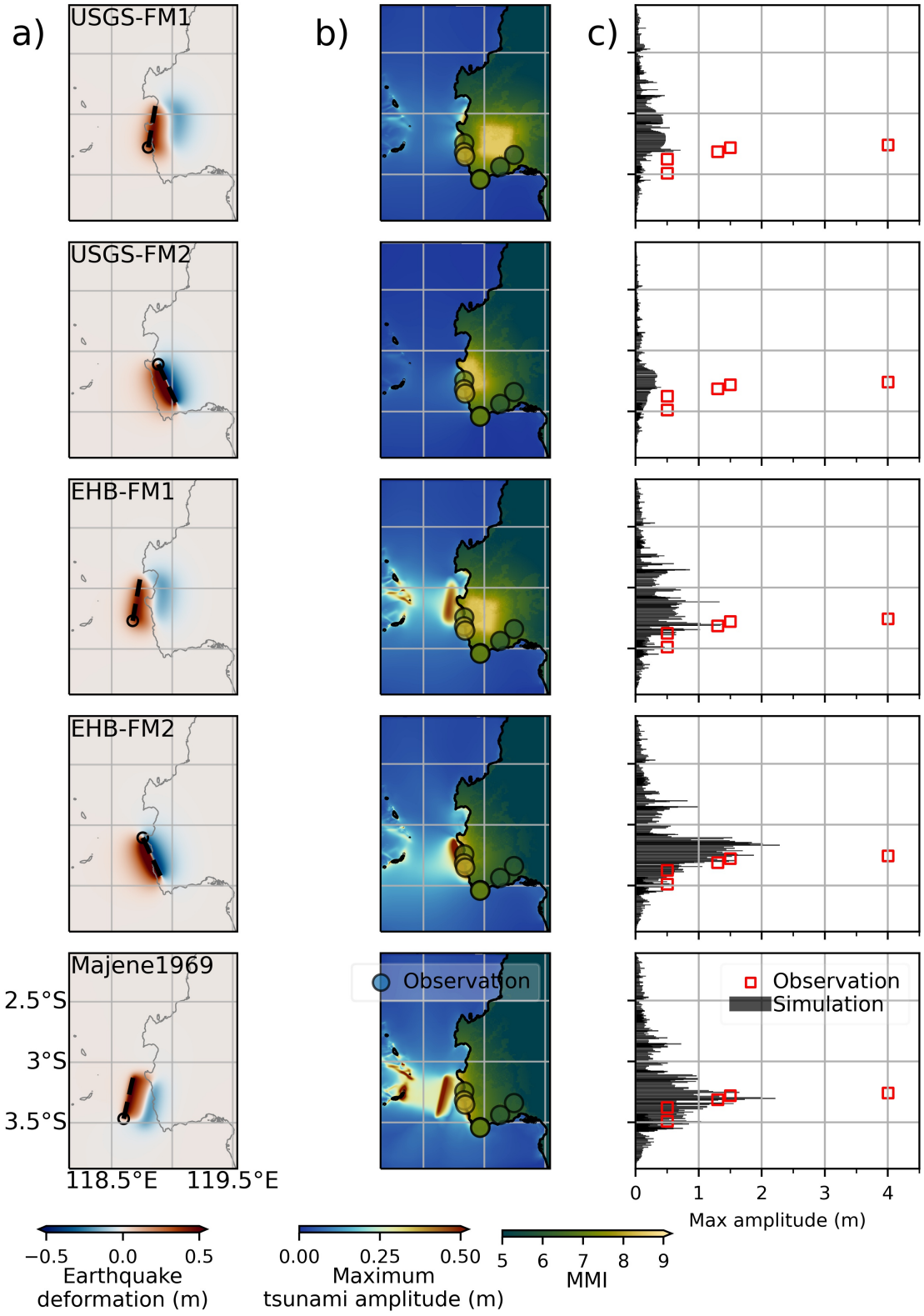

Figure 3. Ground motion (GM) and tsunami modelling of selected scenarios. a) Earthquake deformation model; dashed line and hollow circle indicate fault plane surface projection and coordinate shown in Table 1, respectively. b) GM and maximum tsunami modelling results. c) Maximum simulated tsunami coastal height and tsunami observation.

References

[1] Hall R. Australia–SE Asia collision: plate tectonics and crustal flow. *Geological Society, London, Special Publications* 2011;**355**:75–109. https://doi.org/10.1144/SP355.5.
[2] Cipta A, Robiana R, Griffin J D, Horspool N, Hidayati S, Cummins P R. A probabilistic seismic hazard assessment for Sulawesi, Indonesia. *Geological Society, London, Special Publications* 2016;**441**:133–152. https://doi.org/10.1144/sp441.6.
[3] Prasetya G, De Lange W, Healy T. The Makassar Strait tsunamigenic region, Indonesia. *Natural Hazards* 2001;**24**:295–307. https://doi.org/10.1023/a:1012297413280.
[4] Horspool N, Pranantyo I, Griffin J, Latief H, Natawidjaja D, Kongko W, Cipta A, Bustaman B, Anugrah S, Thio H. A probabilistic tsunami hazard assessment for Indonesia. *Natural Hazards and Earth System Sciences* 2014;**14**:3105–3122. https://doi.org/10.5194/nhess-14-3105-2014.
[5] ITIC. International Tsunami Information Center Newsletter. vol. 2, PO.BOX 3887, Honolulu, Hawaii 96812 USA: ITIC; 1969, p. 8.
[6] ITIC. International Tsunami Information Center Newsletter. vol. 3, PO.BOX 3887, Honolulu, Hawaii 96812 USA: ITIC; 1969, p. 8.
[7] Griffin J, Nguyen N, Cummins P, Cipta A. Historical Earthquakes of the Eastern Sunda Arc: Source Mechanisms and Intensity-Based Testing of Indonesia's National Seismic Hazard Assessment. *Bulletin of the Seismological Society of America* 2018;**109**:43–65. https://doi.org/10.1785/0120180085.
[8] Pranantyo I R, Cummins P R. The 1674 Ambon tsunami: Extreme run-up caused by an earthquake-triggered landslide. *Pure and Applied Geophysics* 2019;**177**:1639–1657. https://doi.org/10.1007/s00024-019-02390-2.
[9] Cummins P R, Pranantyo I R, Pownall J M, Griffin J D, Meilano I, Zhao S. Earthquakes and tsunamis caused by low-angle normal faulting in the Banda Sea, Indonesia. *Nature Geoscience* 2020;**13**:312–318. https://doi.org/10.1038/s41561-020-0545-x.
[10] Soloviev S, Go C, Kim X. *Catalog of tsunamis in the Pacific Ocean*, 1969-1982. Moscow, MGC, 163p 1986.
[11] Soetardjo, Untung M, Arnold E P, Soetadji R, Ismail S, Kertapati E K. *Indonesia*. vol. V. U.S. Geological survey; 1985.
[12] Fikrie M, Hardiansya A. Lembong tallu dan gempa bertubi-tubi di Mamasa 2018. https://lokadata.id/artikel/lembong-tallu-dan-gempa-bertubi-tubi-di-mamasa, last accessed 5 October 2020.
[13] Weston J, Engdahl E R, Harris J, Giacomo D D, Storchak D A. ISC-EHB: reconstruction of a robust earthquake data set. *Geophysical Journal International* 2018;**214**:474–484. https://doi.org/10.1093/gji/ggy155.
[14] Havskov J, Ottemöller L. SeisAn Earthquake Analysis Software. *Seismological Research Letter*s 1999;**70**:532–534. https://doi.org/10.1785/gssrl.70.5.532.
[15] Havskov J, Voss P H, Ottemöller L. Seismological Observatory Software: 30 Yr of SEISAN. *Seismological Research Letters* 2020;**91**:1846–1852. https://doi.org/10.1785/0220190313.
[16] Kennet B L N. IASPEI 1991 Seismological Tables. *Terra Nova* 1991;**3**:122. https://doi.org/10.1111/j.1365-3121.1991.tb00863.x.
[17] Reasenberg P A. FPFIT, FPPLOT, and FPPAGE: Fortran computer programs for calculating and displaying earthquake fault-plane solutions. US Geol. Surv. Open-File Rep. 1985:85–739.
[18] Pagani M, Monelli D, Weatherill G, Danciu L, Crowley H, Silva V, Henshaw P, Butler L, Nastasi M, Panzeri L, Simionato M, Vigano D. OpenQuake Engine: An Open Hazard (and Risk) Software for the Global Earthquake Model. *Seismological Research Letters* 2014;**85**:692–702. https://doi.org/10.1785/0220130087.
[19] Boore D M, Stewart J P, Seyhan E, Atkinson G M. NGA-West2 equations for predicting PGA, PGV, and 5% damped PSA for shallow crustal earthquakes. *Earthquake Spectra* 2014;**30**:1057–1085.
[20] Worden C B, Gerstenberger M C, Rhoades D A, Wald D J. Probabilistic Relationships between Ground-Motion Parameters and Modified Mercalli Intensity in California. *Bulletin of the Seismological Society of America* 2012;102:204–221. https://doi.org/10.1785/0120110156.
[21] Baba T, Takahashi N, Kaneda Y, Ando K, Matsuoka D, Kato T. Parallel Implementation of Dispersive Tsunami Wave Modeling with a Nesting Algorithm for the 2011 Tohoku Tsunami. *Pure and Applied Geophysics* 2015;**172**:3455–3472. https://doi.org/10.1007/s00024-015-1049-2.
[22] Wells D L, Coppersmith K J. New empirical relationships among magnitude, rupture length, rupture width, rupture area, and surface displacement. *Bulletin of the seismological Society of America* 1994;**84**:974–1002.